ASTROBIOLOGY
Volume 19, Number 11, 2019
© Mary Ann Liebert, Inc.
DOI: 10.1089/ast.2018.1997

Investigating the Effect of Perchlorate on Flight-like Gas Chromatography–Mass Spectrometry as Performed by MOMA on board the ExoMars 2020 Rover

Helge Mißbach,[1,2] Harald Steininger,[2,3] Volker Thiel,[1] and Walter Goetz[2]

Downloaded by MPI Sonnensystemforschung MPI 359 from www.liebertpub.com at 04/05/20. For personal use only.

Abstract

The Mars Organic Molecule Analyzer (MOMA) instrument on board ESA's ExoMars 2020 rover will be essential in the search for organic matter. MOMA applies gas chromatography–mass spectrometry (GC-MS) techniques that rely on thermal volatilization. Problematically, perchlorates and chlorates in martian soils and rocks become highly reactive during heating (>200°C) and can lead to oxidation and chlorination of organic compounds, potentially rendering them unidentifiable. Here, we analyzed a synthetic sample (alkanols and alkanoic acids on silica gel) and a Silurian chert with and without Mg-perchlorate to evaluate the applicability of MOMA-like GC-MS techniques to different sample types and assess the impact of perchlorate. We used a MOMA flight analog system coupled to a commercial GC-MS to perform MOMA-like pyrolysis, *in situ* derivatization, and *in situ* thermochemolysis. We show that pyrolysis can provide a sufficient overview of the organic inventory but is strongly affected by the presence of perchlorates. *In situ* derivatization facilitates the identification of functionalized organics but showed low efficiency for *n*-alkanoic acids. Thermochemolysis is shown to be an effective technique for the identification of both refractory and functional compounds. Most importantly, this technique was barely affected by perchlorates. Therefore, MOMA GC-MS analyses of martian surface/subsurface material may be less affected by perchlorates than commonly thought, in particular when applying the full range of available MOMA GC-MS techniques. Key Words: Mars Organic Molecule Analyzer (MOMA)—ExoMars rover—Pyrolysis—Thermochemolysis—Perchlorate—Organics. Astrobiology 19, 1339–1352.

1. Introduction

After four decades of Mars exploration, beginning with the Viking Landers in 1976 (Biemann *et al.,* 1977; ten Kate, 2010; Goetz *et al.,* 2016; Levin and Straat, 2016), the search for biosignatures indicating past or present life is still a key objective for future robotic missions to the martian surface (Westall *et al.,* 2015; Vago *et al.,* 2017). One of the next missions is ESA's ExoMars rover Rosalind Franklin that will be launched in 2020. A variety of onboard optical and analytical instruments will perform a broad search for morphological and chemical biosignatures and analyze geological context information on the surface and in the near subsurface of Mars (2 m depth, with the help of a drilling device; Vago *et al.,* 2017). The Mars Organic Molecule Analyzer (MOMA; Goesmann *et al.,* 2017) is the largest instrument on the rover and the key instrument to detect molecular biosignatures. Together with an infrared spectrometer (MicrOmega; Bibring *et al.,* 2017) and a Raman Laser Spectrometer (RLS; Rull *et al.,* 2017), it makes up the rover's analytical laboratory for a detailed investigation of martian sediments (Vago *et al.,* 2017).

MOMA will examine martian samples by laser desorption/ionization mass spectrometry (LDMS) or gas chromatography–mass spectrometry (GC-MS) (Goesmann *et al.,* 2017; Li *et al.,* 2017). GC-MS provides the opportunity to separate and identify organics with high sensitivity and is therefore well suited to search for molecular biosignatures in extraterrestrial samples (Summons *et al.,* 2008). Lately, the SAM (Sample Analysis at Mars) instrument on board the Curiosity rover demonstrated that GC-MS is a powerful tool to detect low-molecular-weight organics in martian surface sediments (Mahaffy *et al.,* 2012; Freissinet *et al.,* 2015; Eigenbrode *et al.,* 2018). MOMA GC-MS has three different operational modes, that of pyrolysis (thermal volatilization), *in situ* derivatization, and *in situ* thermochemolysis (on-line

[1]Geobiology, Geoscience Centre, University of Goettingen, Goettingen, Germany.
[2]Max Planck Institute for Solar System Research, Goettingen, Germany.
[3]OHB System AG, Weßling-Oberpfaffenhofen, Germany.

Downloaded by MPI Sonnensystemforschung MPI 359 from www.liebertpub.com at 04/05/20. For personal use only.

methylation). The latter operational modes are completed by thermal desorption of the derivatized organics from crushed sample material. These techniques are designed to facilitate the analysis of polar compounds (*e.g.,* alkanols, fatty acids, amino acids) in GC-MS and, in the case of thermochemolysis, to limit destruction of refractory organics at higher temperatures (Challinor, 2001; Rodier *et al.,* 2005; Buch *et al.,* 2006; Geffroy-Rodier *et al.,* 2009; Zaikin and Halket, 2009). A detailed description of the MOMA GC-MS system and its operational modes is given in the work of Goesmann *et al.* (2017).

Organic signatures in martian sediments can potentially derive from biological (*i.e.,* past or present life) or from abiotic sources, as for example meteorites or *in situ* abiotic synthesis (Flynn, 1996; Shock and Schulte, 1998; Botta and Bada, 2002; McCollom and Seewald, 2007; Summons *et al.,* 2011; Konn *et al.,* 2015; Westall *et al.,* 2015). Therefore, it is crucial to determine whether any organic molecules found on Mars derive from abiotic or biological sources, for example by looking for specific distribution patterns of organic compounds, stable isotope patterns, or enantiomeric excess (Meierhenrich, 2008; Summons *et al.,* 2008; Cady and Noffke, 2009; Westall *et al.,* 2015; Vago *et al.,* 2017). Especially lipid biomarkers have the potential to be preserved over geological timescales (Brocks and Summons, 2004; Summons, 2014). However, discrimination between abiotic and biologically derived organics can be hampered by degradation of organic molecules, for example via thermal alteration or radiation (Oró and Holzer, 1979; Brocks and Summons, 2004; Peters *et al.,* 2005; Kminek and Bada, 2006; Pavlov *et al.,* 2012; Mißbach *et al.,* 2016). On the martian surface and in the near subsurface, organic compounds are degraded by solar and galactic cosmic rays. These processes encompass primary (*i.e.,* impact fragmentation) or secondary effects (oxidation by O or HO radicals generated from particle impacts with the mineral matrix; Pavlov *et al.,* 2012).

The ExoMars rover's capability to collect samples from 2 m depth allows obtaining martian sediments that were protected from radiation and thus, potentially, preserved organic matter (Westall *et al.,* 2015; Goetz *et al.,* 2016; Vago *et al.,* 2017). However, analysis of these potential organics can be further complicated by the presence of oxychlorine compounds (*e.g.,* Ca- and Mg-perchlorates and chlorates, hereafter focusing mainly on perchlorates) in martian sediments whose presence was revealed by the Phoenix Mars lander and the Mars Science Laboratory (MSL) rover (Hecht *et al.,* 2009; Kounaves *et al.,* 2010, 2014; Glavin *et al.,* 2013; Sutter *et al.,* 2017a). Reevaluation of Viking results (Biemann *et al.,* 1976, 1977) suggested that perchlorates were also present at Viking landing sites, although these results were questioned and intensively discussed (Navarro-González *et al.,* 2010, 2011; Biemann and Bada, 2011; Navarro-González and McKay, 2011; Guzman *et al.,* 2018). The interference of perchlorates in pyrolysis measurements of martian sediments is known from SAM analysis (Glavin *et al.,* 2013; Freissinet *et al.,* 2015). Perchlorates are relatively inactive at low temperatures (*i.e.,* martian surface temperatures) and thus, for example, remain unreacted in soils (Brown and Gu, 2006; Catling *et al.,* 2010). However, they become reactive during heating, as the perchlorate molecule decomposes in the temperature range of 200–600°C, forming products likely leading to oxidation and chlorination of organic compounds (Navarro-González *et al.,* 2010, 2011; Steininger *et al.,* 2012; Sephton *et al.,* 2014). Potential biosignatures may therefore be destroyed in the presence of perchlorates, either by chemical alteration or complete combustion (*i.e.,* transformation into CO_2; Steininger *et al.,* 2012).

Analog studies are necessary to determine analytical limits and pitfalls; hence, they are an essential prerequisite to support data interpretation for upcoming missions. In this study, we analyzed two different samples (a synthetic standard mix with alkanols and alkanoic acids on silica gel and a Silurian chert) with addition of different amounts of perchlorate. We used a MOMA flight analog system (FAS) coupled to a commercial GC-MS and MOMA-like pyrolysis and *in situ* derivatization/thermochemolysis techniques. The study aims at (i) evaluating the applicability of MOMA-like GC-MS techniques on different sample types, (ii) assessing the impact of Mg-perchlorates on organics during heating, and (iii) providing reference data for interpretation of MOMA data to be acquired during surface operations. Our results demonstrate that especially thermochemolysis with tetramethylammonium hydroxide (TMAH) is a powerful technique to determine different organics in perchlorate-rich samples.

2. Materials and Methods

2.1. Samples

Two samples were used in this study. The first sample was a standard mixture consisting of

- primary alkanols (n-C_{11}–n-C_{13} alkan-1-ols)
- alkanoic acids (n-C_{11}–n-C_{13})
- secondary alkanols (n-C_{11} and n-C_{12} alkan-2-ols)

in decreasing molar abundances (Table S.1; Supplementary Material is available online at www.liebertonline.com/ast). Compounds with relatively shorter carbon chain lengths were used (i) because MOMA GC-MS is explicitly targeting shorter-range compounds and (ii) to clearly differentiate between compounds from the standard mix and highly abundant biological compounds (*e.g.,* C_{16} and C_{18} alkanoic acids) which are typical contamination in derivatization agents and/or the lab environment. The mixture was deposited on SiO_2 (silica gel; precleaned at 550°C for >3 h). These compounds represent main compound classes potentially resulting from abiotic synthesis (McCollom *et al.,* 1999; Rushdi and Simoneit, 2001; Mißbach *et al.,* 2018) as well as important biologically produced lipids that will be targeted by ExoMars and MOMA (Goesmann *et al.,* 2017; Vago *et al.,* 2017).

The second sample was a silica-rich Silurian black chert from the Holy Cross Mountains in central Poland (for details see Kremer, 2005; Kremer and Kazmierczak, 2005), containing ~0.5 wt % total organic carbon. This sample was also used in earlier work (Goesmann *et al.,* 2017, their Chapter 7.5) and is included in our study as a natural reference. The selection of silica-rich samples for this study was motivated by the detection of silica phases in Oxia Planum, the ExoMars 2020 landing site (Carter *et al.,* 2016; Bridges *et al.,* 2017). Organic matter trapped in opaline silica has a high preservation potential (as *e.g.,* shown for Archean cherts) and is thus a high-priority astrobiology target for the ExoMars 2020 mission

Downloaded by MPI Sonnensystemforschung MPI 359 from www.liebertpub.com at 04/05/20. For personal use only.

(Marshall *et al.,* 2007; Westall *et al.,* 2015; Duda *et al.,* 2016, 2018). Before analysis, the rock pieces were manually powdered with a mortar that had been intensively rinsed with isopropanol and dried prior to use. A higher organic content of the samples compared to martian sediments (mg/g vs. ng/g, respectively) has been used in our experiment to ensure a clear distinction between signals from the samples and background/contamination.

For this study, magnesium perchlorate (Mg-perchlorate) was used to test the effects of perchlorates on MOMA-like GC-MS techniques. Mg-perchlorate concentrations were adjusted to circa 1 wt % and circa 10 wt %, the former representing concentrations close to those detected on Mars (Hecht *et al.,* 2009; Glavin *et al.,* 2013), the latter being a worst-case scenario. Perchlorates are highly mobile in water (Brown and Gu, 2006). Therefore, local enrichment of perchlorates via formation of salt brines in subsurface areas is possible (Cull *et al.,* 2010; Martín-Torres *et al.,* 2015). Depending on the desired concentration, perchlorate was added to the sample in different ways. For samples with 1 wt % perchlorate content, the perchlorate was first mixed with precleaned (550°C for >3 h) and powdered (pebble mill) sea sand and afterward mixed with the sample in the correct ratio. This step enables an easier and more exact handling of small amounts of perchlorate. Pure Mg-perchlorate was mixed with the samples to reach 10 wt % perchlorate content.

2.2. MOMA FAS and experimental procedure

The experiments were performed with a MOMA FAS connected to a commercial GC-MS (Section 2.3; see also Goesmann *et al.,* 2017). The FAS consists of a MOMA oven, an adsorption trap (filled with Tenax® GR; see Goesmann *et al.,* 2017, for details), and a tapping station including all the tubing to connect the different parts with the GC-MS (Fig. 1). All transfer lines were heated to circa 110°C.

The analyses in this study were performed as close as possible to MOMA conditions. However, there are differences to the MOMA flight GC-MS instrument and the basic procedures, as they had to be transferred to a laboratory configuration. The major differences are as follows. (i) The maximum temperatures of the transfer lines and the adsorption trap are lower in the FAS compared to those planned for the MOMA flight instrument (transfer lines: 110°C vs. 135°C, trap: 160°C vs. max. 300°C, respectively). These lower temperatures most certainly hamper the transfer of compounds with higher boiling points to the GC-MS. (ii) The adsorption trap in the FAS does not support flow inversion, so that volatiles have to pass through the whole trap on their way to the GC. This increases the chance of cross contamination between samples. (iii) Less derivatization agent was used (3.5 µL vs. 15 µL in MOMA), and it was added to the cold sample before heating, instead of being released from derivatization capsules at elevated temperatures. A detailed discussion on this matter and the exact MOMA GC-MS conditions are given in the work of Goesmann *et al.* (2017).

For every analysis, between 3.5 and 4 mg of sample was used. If applicable, the sample was mixed with circa 1 mg perchlorate mix (Section 2.1) or circa 0.5 mg pure perchlorate (aiming for 1 wt % or 10 wt % Mg-perchlorate, respectively). After transferring the sample to the oven, it was dried at 80°C for 10 min, leaving the oven unconnected to the tapping station. For *in situ* derivatization and thermochemolysis, 3.5 µL of the respective reagent was added to the dry sample. According to Goesmann *et al.* (2017), the following reagents were used:

- *N,N*-methyl-tert-butyl-dimethylsilyltrifluoroacetamide (MTBSTFA; >97%, Sigma-Aldrich) with *N,N*-dimethylformamide (DMF; >99.5%, Thermo Scientific) in a 3:1 (v:v) mixture, while DMF is added to increase derivatization efficiency (Buch *et al.,* 2006)
- *N,N*-dimethylformamide dimethyl acetal (DMF-DMA; Sigma-Aldrich)
- Tetramethylammonium hydroxide (TMAH, 25 wt % in methanol; Sigma-Aldrich)

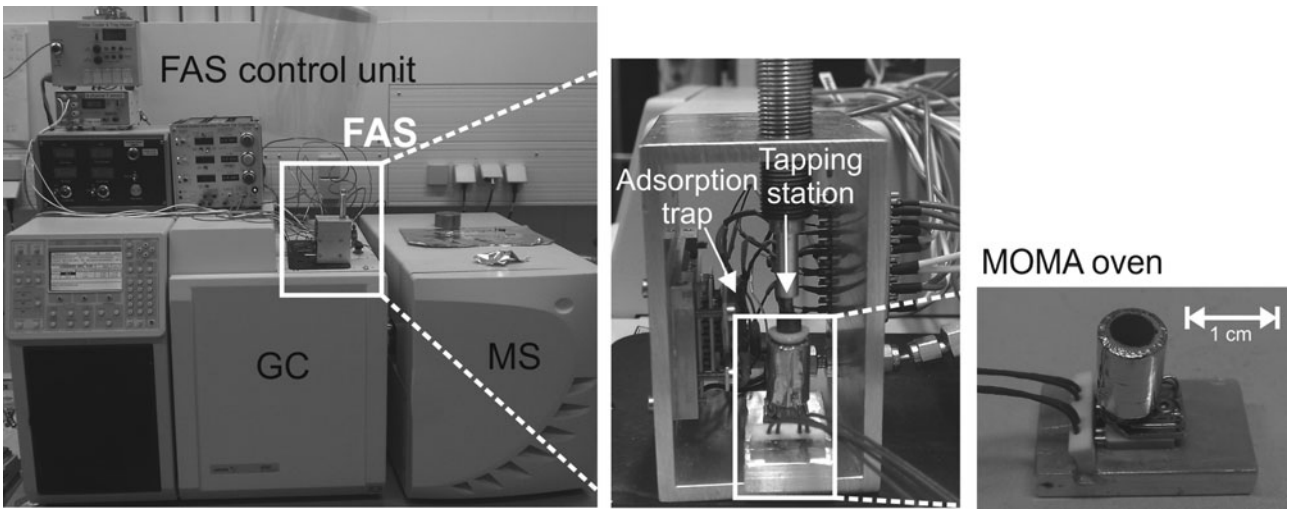

FIG. 1. The flight analog system (FAS) mounted on the gas chromatograph (GC; left), view inside the FAS with adsorption trap and tapping station that seals the oven (center), and the oven separated from the tapping station (right). MS = mass spectrometer.

Downloaded by MPI Sonnensystemforschung MPI 359 from www.liebertpub.com at 04/05/20. For personal use only.

MTBSTFA/DMF and DMF-DMA were used for *in situ* derivatization; TMAH was used for *in situ* thermochemolysis. All three reagents will be available in the MOMA instrument. MTBSTFA and TMAH are also available in the SAM instrument on board the Curiosity rover (Mahaffy *et al.,* 2012).

After connecting the oven to the tapping station, the adsorption trap was cooled to 0°C by a Peltier element. Pyrolysis was performed directly as a single heating step to 700°C for 10 s. The heating rate of the oven was circa 300°C/min. Reaction temperatures and times for *in situ* derivatization/thermochemolysis with MTBSTFA/DMF, DMF-DMA, and TMAH were the following: 250°C for 10 min, 140°C for 4 min, and 600°C for 40 s, respectively. Flash heating of the adsorption trap to 160°C (circa 200°C/min) was initiated immediately afterward to release volatiles into the GC-MS, which was started in parallel. Slight fluctuations of the heating rate of the adsorption trap and temperature of transfer lines between the runs influenced the release of compounds from the adsorption trap and led to variations in the retention times of compounds in the range of 0.1–0.3 min.

Each analysis using a given sample and set of parameters was carried out at least twice to validate reproducibility. Multiple cleaning runs and system blank analyses were carried out between the sample runs to control cross contamination. Furthermore, blank analyses of Mg-perchlorate and all wet chemistry reagents were conducted. All blank analyses were carried out in pyrolysis mode.

2.3. GC-MS parameters

A Varian 3800 GC (gas chromatograph) coupled to a Varian 240-MS (mass spectrometer) was used for this study. The GC was equipped with a capillary column (Agilent J&W VF-5ms; 30 m length, 0.25 mm inner diameter, 0.25 µm film thickness). This column has similar properties as the Restek MXT-5 used in the MOMA instrument (Goesmann *et al.,* 2017). The carrier gas (helium) flow was set to 2 mL/min. The injector temperature was 250°C, and the split ratio was set to 30. The GC oven was heated from 30°C (isotherm for 1 min) to 250°C (isotherm for 5 min) with 10°C/min. The (solvent) delay for acquisition of mass spectra was 1 min for pyrolysis, 10 min for MTBSTFA/DMF, 8 min for DMF-DMA, and 7 min for TMAH. Recording of full scan mass spectra proceeded in fast scan mode with a scan time of 0.58 s and a mass range from *m/z* 35 to 1000. Compounds were determined by comparison to reference spectra (NIST mass spectral library). *n*-Alkenes were also identified by their elution order (Nierop and van Bergen, 2002).

3. Results

3.1. Blanks

The system blanks showed traces of contamination, mostly in the form of siloxanes (*e.g.,* column degradation), phthalates (*e.g.,* from plasticizers from transport boxes, vial caps), silanes and DMF (carryover from previous runs with derivatization agents, Fig. S.1a). Additionally, traces of cross contamination in varying composition from earlier analyses of different samples were detected in some of the runs (*e.g.,* chloroalkanes and sulfur).

Table 1. Aromatic Hydrocarbons, Chlorinated and Nitrogen-Bearing Compounds Originating from MOMA-like Pyrolysis and *In Situ* Thermochemolysis

Peak label	*Compound*	*Chemical formula*
Aromatic hydrocarbons		
A(I)	Benzene	C_6H_6
A(II)	Toluene	C_7H_8
A(III)	Xylenes	C_8H_{10}
A(IV)	Trimethylbenzenes	C_9H_{12}
A(V)	1-Propynyl-benzene (tentatively identified)	C_9H_8
A(VI)	Naphthalene	$C_{10}H_8$
A(VII)	Methylnaphthalenes	$C_{11}H_{10}$
A(VIII)	Dimethylnaphthalenes	$C_{12}H_{12}$
A(IX)	Acenaphthylene	$C_{12}H_8$
A(X)	Fluorene	$C_{13}H_{10}$
A(XI)	Phenanthrene	$C_{14}H_{10}$
Chlorinated compounds		
Cl(I)	Chloroethene	C_2H_3Cl
Cl(II)	Dichloromethane	CH_2Cl_2
Cl(III)	Trichloromethane	$CHCl_3$
Cl(IV)	Carbon tetrachloride	CCl_4
Cl(V)	Trichloroacetonitrile (tentatively identified)	C_2Cl_3N
Cl(VI)	Trichloroethylene	C_2HCl_3
Cl(VII)	Chloral hydrate	$C_2H_3Cl_3O_2$
Cl(VIII)	Tetrachloroethylene	C_2Cl_4
Cl(IX)	Chlorobenzene	C_6H_5Cl
Cl(X)	Benzoyl chloride (tentatively identified)	C_7H_5ClO
Cl(XI)	2-Chloronicotinonitrile (tentatively identified)	$C_6H_3ClN_2$
Cl(XII)	Trichlorobenzenes	$C_6H_3Cl_3$
Cl(XIII)	Tetrachlorobenzenes	$C_6H_2Cl_4$
Cl(XIV)	Pentachlorobenzene	C_6HCl_5
Cl(XV)	Hexachlorobenzene	C_6Cl_6
Cl(XVI)	Pentachlorobenzonitrile (tentatively identified)	C_7Cl_5N
N-bearing compounds		
N(I)	Benzonitrile	C_7H_5N
N(II)	Pyridinecarbonitrile	$C_6H_4N_2$
N(III)	1,5-Dicyano-2,4-dimethyl-2,4-diazapentane	$C_7H_{12}N_4$
N(IV)	2,3-Dimethylpyrazine	$C_6H_8N_2$
N(V)	1,3-Dimethyl-2,4,5-trioxoimidazolidine	$C_5H_6N_2O_3$
N(VI)	Naphthalenecarbonitrile	$C_{11}H_7N$

The perchlorate blank showed a variety of chlorinated organics, including chloroethene, carbon tetrachloride, pentachlorobenzene, and hexachlorobenzene (Fig. S.1b; Table 1). Furthermore, compounds bearing both nitrogen and chlorine were detected. Formation of these compounds might be explained by the reaction of chlorine with N-bearing compounds (*e.g.,* DMF carryover, see above and Fig. S.1a).

3.2. Pyrolysis

Pyrolysis of the standard mixture (see Section 2.1) in the FAS yielded *n*-alkenes (including *n*-alk-1-enes, *n*-alk-2-enes, and midchain alkenes) and *n*-alkanals, with C_{11}–C_{13} *n*-alk-1-enes being the main compounds (Fig. 2a). Furthermore, small

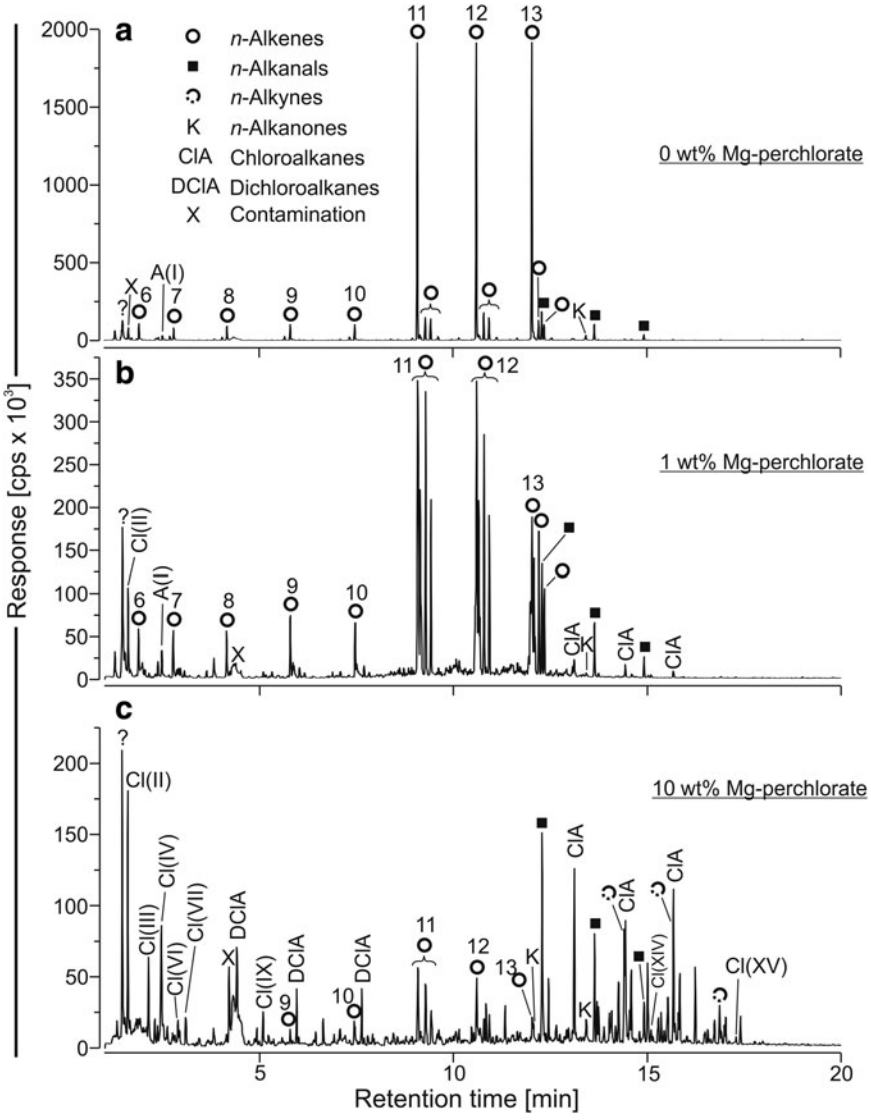

FIG. 2. GC-MS chromatograms (total ion current) of the pyrolysates obtained from the standard mixture: (**a**) 0 wt % Mg-perchlorate; (**b**) 1 wt % Mg-perchlorate; (**c**) 10 wt % Mg-perchlorate. Numbers indicate the carbon chain lengths of corresponding *n*-alkenes. Peak labels with roman numerals denote aromatic (A) and chlorinated (Cl) compounds as given in Table 1. cps = counts per second. Note that none of the functionalized compounds from the standard mixture (*i.e.,* *n*-alkanols or *n*-alkanoic acids) can be identified. Degradation (especially of *n*-alkenes) and formation of chlorinated compounds increases from (a) to (c). Several compounds in (c) could not be identified, as mass spectra were undiagnostic (major unlabeled peaks).

relative amounts of *n*-alkanones and benzene were detected. None of the functionalized compounds initially present in the standard mix were observed. Addition of 1 wt % of Mg-perchlorate to the standard mixture led to the same distribution of compounds (Fig. 2b). However, considerably lower amounts of *n*-alk-1-enes were detected (note different *y*-axis ranges in Fig. 2a–2c), whereas other *n*-alkene moieties and *n*-alkanals increased in their relative abundance. In addition, the formation of minor chloroalkanes was observed. Addition of 10 wt % Mg-perchlorate to the standard mixture resulted in a further substantial decrease in *n*-alkenes, whereas *n*-alkanals increased in their relative abundance. Additionally, *n*-alkynes were observed. A major feature is the dominant appearance of chlorinated compounds such as chloroalkanes, dichloroalkanes, dichloromethane, and chlorobenzene (Fig. 2c).

Pyrolysis of the black chert revealed *n*-alkenes (C_5–C_{20}), *n*-alkanes (C_7–C_{21}), and a variety of aromatic hydrocarbons (*e.g.,* benzene, toluene, xylenes, naphthalene, phenanthrene; Fig. 3a). Analysis of the sample with 1 wt % of Mg-perchlorate resulted in a roughly similar compound distribution. Nevertheless, a lower overall abundance of aliphatic versus aromatic hydrocarbons and a shorter range of *n*-alkenes (C_5–C_{16}) were clearly observed (Fig. 3b). The pyrolysis experiment of the black chert with 10 wt % Mg-perchlorate mostly led to chlorinated compounds (*e.g.,* carbon tetrachloride, chloral hydrate, chlorobenzenes; Fig. 3c). The only aromatic hydrocarbon observed was toluene. No aliphatic hydrocarbons were detected. Some of the chlorinated compounds identified in this run were also detected in the perchlorate blank but in much lower amounts (Fig. S.1b).

3.3. Derivatization with MTBSTFA/DMF and DMF-DMA

In situ derivatization of *n*-alkanols and *n*-alkanoic acids from the standard mixture with MTBSTFA/DMF resulted in *tert*-butyldimethylsilyl ethers and esters, respectively (Fig. S.2a). However, only the *n*-alkanols showed a satisfactory derivatization, whereas *n*-alkanoic acid derivatives were nearly absent (Fig. S.2a). Beside the standard mixture compounds, major contamination introduced from the derivatization reagent was observed. The analysis with 1 wt % of Mg-perchlorate yielded the same compounds with almost the

Downloaded by MPI Sonnensystemforschung MPI 359 from www.liebertpub.com at 04/05/20. For personal use only.

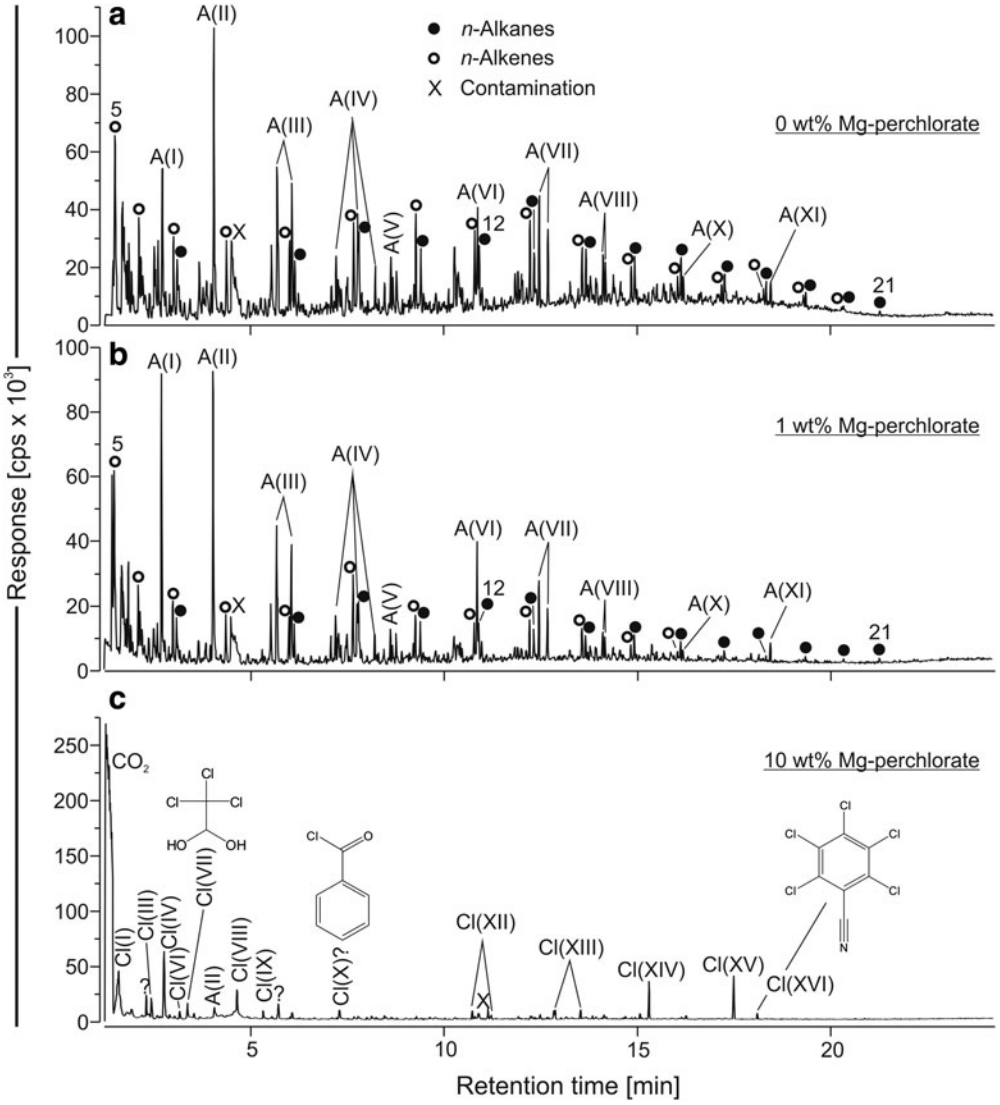

FIG. 3. GC-MS chromatograms (total ion current) of the black chert pyrolysates: (**a**) 0 wt % Mg-perchlorate; (**b**) 1 wt % Mg-perchlorate; (**c**) 10 wt % Mg-perchlorate. Numbers indicate the carbon chain lengths of corresponding *n*-alkenes/*n*-alkanes. Peak labels with roman numerals denote aromatic (A) and chlorinated (Cl) compounds as given in Table 1. cps = counts per second. Note increasing degradation of organic compounds due to Mg-perchlorate addition, as reflected by more pronounced aromatization in (b) and major formation of chlorinated species in (c).

Downloaded by MPI Sonnensystemforschung MPI 359 from www.liebertpub.com at 04/05/20. For personal use only.

same response (Fig. S.2b). Analyses with higher amounts of perchlorate were not carried out (discussed in Section 4.2.2).

After *in situ* derivatization with DMF-DMA, only contamination from the derivatization agent and the system was identified. None of the expected derivatized compounds (*e.g.,* fatty acid methyl esters) have been detected.

3.4. Thermochemolysis with TMAH

All eight compounds from the standard mixture were observed in the expected abundances after *in situ* thermochemolysis (as their corresponding methyl ethers and methyl esters, Fig. 4a). Additionally, high abundances of *n*-C_{11} to *n*-C_{13} alkenes as well as lower amounts of shorter *n*-alkenes, *n*-alk-2-enes, midchain alkenes and *n*-alkanals were observed (Fig. 4a). The same compounds were present after addition of 1 wt % Mg-perchlorate (Fig. 4b). *n*-Alkan-1-ols show the same abundance, whereas most *n*-alkanoic acids, *n*-alkenes, and *n*-alkanals had lower intensities compared to the perchlorate-free analysis (compare Fig. 4a, 4b). Furthermore, chloroalkanes were observed (also present in lower amounts in previous blanks). Thermochemolysis of the standard mixture with 10 wt % Mg-perchlorate revealed the same compounds as for the measurements with 1 wt % Mg-perchlorate, also at similar abundances. Additionally, a variety of nitrogen-bearing compounds were detected, including high amounts of 1,5-dicyano-2,4-dimethyl-2,4-diazapentane (Fig. 4c; Morisson, 2017; NIST mass spectral library).

The chromatogram obtained from the black chert after *in situ* thermochemolysis is similar to the pyrolysis run. The same compounds were detected, albeit with a lower abundance of some aromatics relative to aliphatic hydrocarbons. Additionally, *n*-C_8 to *n*-C_{14} alkanoic acids were detected as their methyl esters (Fig. 5a). Thermochemolysis of the black

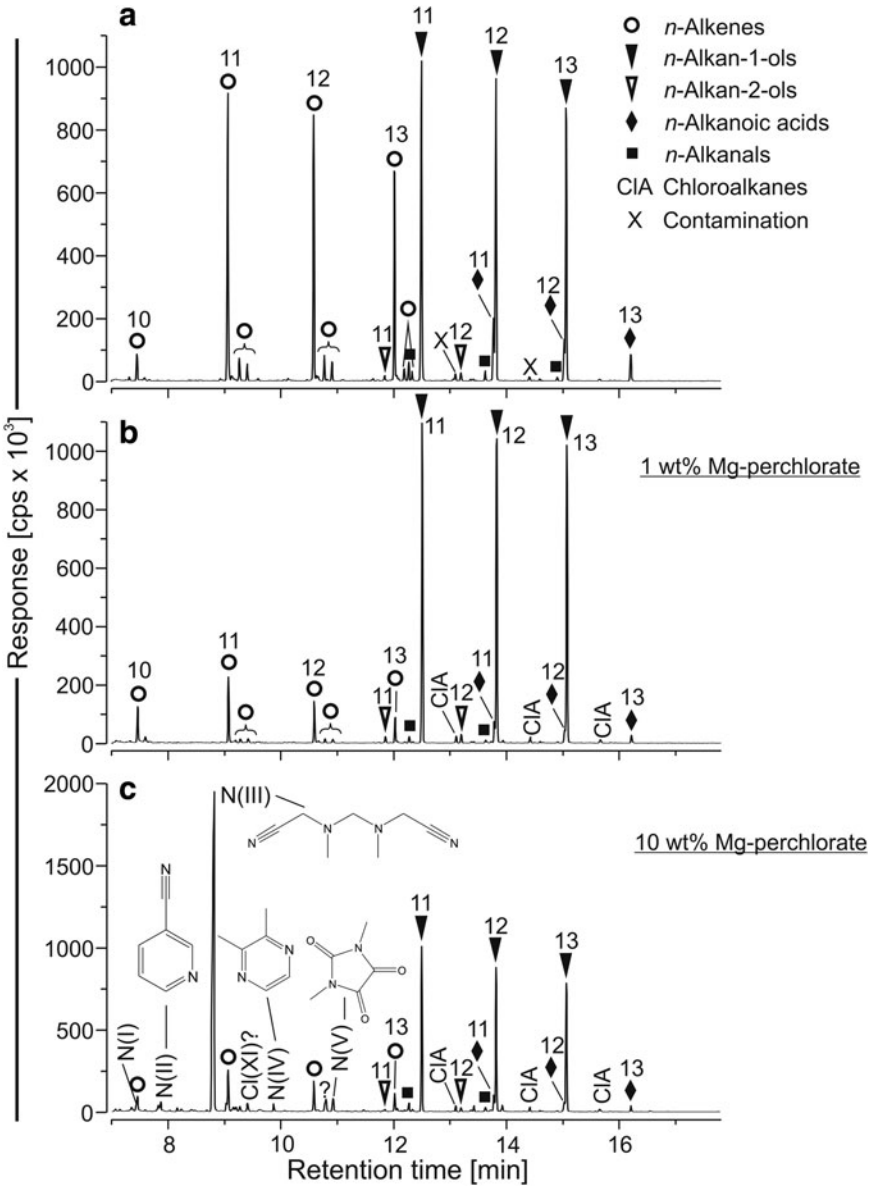

FIG. 4. GC-MS chromatograms (total ion current) of the *in situ* thermochemolysis with TMAH of the standard mixture with (**a**) 0 wt % Mg-perchlorate, (**b**) 1 wt % Mg-perchlorate, and (**c**) 10 wt % Mg-perchlorate. *n*-Alkanols and *n*-alkanoic acids were analyzed as their methyl ethers and esters, respectively. Numbers indicate the carbon chain lengths of corresponding *n*-alkan-1-ols, *n*-alkan-2-ols, *n*-alkanoic acids, and *n*-alkenes. Peak labels with roman numerals denote nitrogen-bearing (N) and chlorinated (Cl) compounds as given in Table 1. cps = counts per second. Note that all compounds from the standard mixture are clearly identifiable in (a) to (c). Thus, Mg-perchlorate does not have a major detrimental effect on these analyses. Note furthermore the appearance of major nitrogen-bearing compounds in (c).

Downloaded by MPI Sonnensystemforschung MPI 359 from www.liebertpub.com at 04/05/20. For personal use only.

chert with 10 wt % Mg-perchlorate led to the same array of aliphatic and aromatic hydrocarbons, compared to the analysis without perchlorate (Fig. 5b). However, some aromatic compounds show higher abundance relative to neighboring aliphatic hydrocarbons (*e.g.,* *n*-alkenes) as, for example, 1-propynyl-benzene (tentatively identified) and naphthalene. Acenaphtylene was identified as a dominant compound that has not been observed in other runs. Identical nitrogen-bearing compounds as observed for the thermochemolysis of the standard mixture with 10 wt % Mg-perchlorate (*e.g.,* benzonitrile, 1,5-dicyano-2,4-dimethyl-2,4-diazapentane) were detected in the analysis of the black chert, although at different relative abundances (Fig. 5b; see also Fig. 4c).

4. Discussion

4.1. Thermal decomposition and possible by-products

Pyrolysis can transform organic compounds via cracking of chemical bonds. The products formed depend on the initial chemical structure but are further controlled by temperature, surrounding gas (or gases), pressure, presence or absence of catalysts, and reaction time (Moldoveanu, 2010).

The virtual absence of the (initially added) functionalized compounds (*n*-alkan-1-ols, *n*-alkan-2-ols, *n*-alkanoic acids) from the pyrolysis products of the standard mixture (Fig. 2a) are results of thermal decomposition. Pyrolysis of an *n*-alkan-1-ol usually leads to the formation of the corresponding *n*-alk-1-ene and *n*-alkanal via dehydration and dehydrogenation, respectively (Moldoveanu, 2010). Furthermore, rearrangement and hydrogen shift accompanying the dehydration reaction can lead to the corresponding *n*-alk-2-ene and various midchain *n*-alkenes. Shorter *n*-alkene moieties are also common products resulting from further fragmentation (Boss and Hazlett, 1976; Nierop and van Bergen, 2002; Moldoveanu, 2010). Secondary alkanols (*e.g.,* alkan-2-ols) principally undergo the same main reactions during pyrolysis, generating *n*-alkenes and *n*-alkanones (Boss and Hazlett, 1976; Moldoveanu, 2010). Pyrolysis

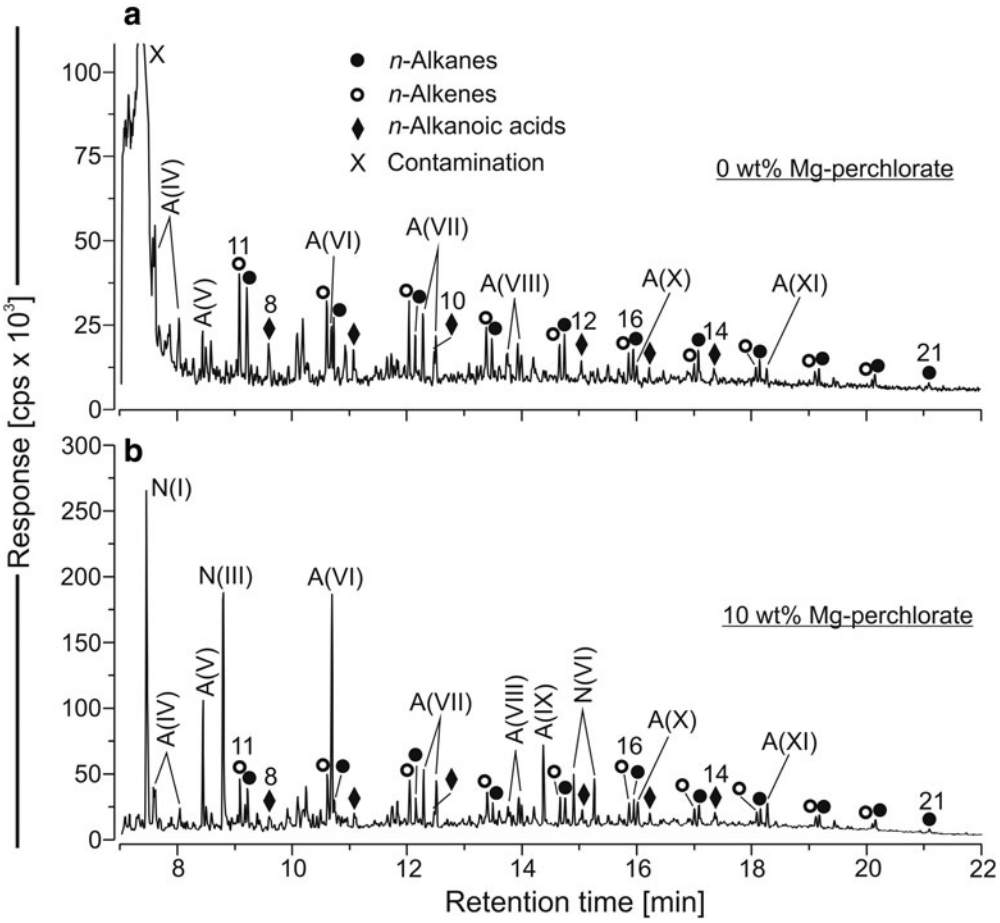

FIG. 5. GC-MS chromatograms (total ion current) of the *in situ* thermochemolysis with TMAH of the black chert: (**a**) 0 wt % Mg-perchlorate; (**b**) 10 wt % Mg-perchlorate. *n*-Alkanoic acids were analyzed as their methyl esters. Numbers indicate the carbon chain lengths of corresponding *n*-alkanoic acids and *n*-alkenes/*n*-alkanes. Peak labels with roman numerals denote aromatic (A) and nitrogen-bearing (N) compounds as given in Table 1. cps = counts per second. Note that all compounds from (a) are clearly identifiable in (b).

products of *n*-alkanoic acids can include *n*-alkanes and *n*-alkenes, mainly due to decarboxylation and dehydration reactions (Nierop and van Bergen, 2002; Moldoveanu, 2010). *n*-Alkenes and *n*-alkanals observed after *in situ* thermochemolysis of the standard mixture are also products of the reactions described above (Fig. 4a).

Dominant aromatic hydrocarbons and *n*-alkene/*n*-alkane doublets were observed after pyrolysis of the black chert (Fig. 3a). The aromatic hydrocarbons potentially derive from the kerogen as a result of cleavage from the macromolecule upon pyrolysis. However, aromatic hydrocarbons can also be formed via cyclization and aromatization reactions of aliphatic hydrocarbons and/or functionalized compounds during pyrolysis (Lockhart *et al.,* 1981; Hartgers *et al.,* 1994, 1995; Moldoveanu, 2010). Hereby, higher temperatures can cause a greater variety of aromatic compounds and thus, potentially, hamper the identification of parent molecules (Moldoveanu, 2010; Morisson, 2017). Furthermore, *n*-alkenes are frequently observed as pyrolysis products from kerogens, leading to typical *n*-alkene/*n*-alkane doublets (Lewan *et al.,* 1979; Burnham *et al.,* 1982; Huizinga *et al.,* 1988). Thus, some of the compounds observed in the pyrolysis and thermochemolysis runs of the black chert might be by-products from high-temperature thermal decomposition (*e.g.,* benzene, toluene, naphthalene, fluorene; Figs. 3a and 5a). In comparison, only one aromatic compound was observed in the pyrolysis of the standard mixture (*i.e.,* benzene; Fig. 2a).

By-products from decomposition of the Tenax trap are also a potential source for hydrocarbon contamination, for example, benzene, toluene, xylene, and naphthalene, as detected in the SAM instrument (Freissinet *et al.,* 2015). A clear distinction between pyrolysis products of the black chert and these contaminants is hardly possible. However, blank runs never showed these by-products (Fig. S.1), and also runs with the standard mixture only revealed traces of these compounds. Hence, most of the aromatic hydrocarbons observed probably derive from kerogen and/or thermal decomposition and aromatization of aliphatic parent organics in the black chert.

4.2. Applicability of different techniques and impact of perchlorate

4.2.1. Pyrolysis. This technique is a simple way to search for organics in soils and surface rocks and has been applied during previous landed missions to Mars (Biemann

Downloaded by MPI Sonnensystemforschung MPI 359 from www.liebertpub.com at 04/05/20. For personal use only.

Downloaded by MPI Sonnensystemforschung MPI 359 from www.liebertpub.com at 04/05/20. For personal use only.

et al., 1976, 1977; Sutter *et al.,* 2012; Glavin *et al.,* 2013; Freissinet *et al.,* 2015). Furthermore, it is widely applied to study refractory organics that are bound to kerogen (Vandenbroucke and Largeau, 2007; Hallmann *et al.,* 2011). However, an identification of (intact) functional compounds through pyrolysis with the given setup and parameters was not possible, as demonstrated by the experiments using the standard mixture (Fig. 2a). Thus, this approach is not ideally suited for the analysis of functional compounds but rather for more complex macromolecular materials (see below).

Pyrolysis of the black chert without Mg-perchlorate seems to give a sufficient overview of the organic inventory of the sample. However, high-temperature pyrolysis of the black chert produced aromatic and unsaturated hydrocarbons that do not necessarily reflect the true inventory of organic compounds in the sample (see discussion in Section 4.1). Here, overall lower pyrolysis temperatures or a stepwise approach (presented in Goesmann *et al.,* 2017) might be possibilities to minimize analytical by-products.

While all compounds were still clearly identifiable in pyrolysis mode after the addition of 1 wt % Mg-perchlorate, the addition of 10 wt % Mg-perchlorate led to degradation of existing organics and formation of major amounts of chlorinated hydrocarbons (Figs. 2b, 2c and 3b, 3c). This is well in line with earlier observations (Steininger *et al.,* 2012). Decomposition of Mg-perchlorate leads to formation of MgO and $MgCl_2$ as well as O_2 and Cl_2, or their associated radicals (Manelis *et al.,* 2003; Navarro-González *et al.,* 2010, 2011; Steininger *et al.,* 2012). O and Cl radicals further lead to the formation of CO_2 from organic matter and chlorinated organic compounds via oxidation and chlorination, respectively (Sephton *et al.,* 2014). A determination of exact parent molecules of chlorinated compounds observed in our study is difficult, if not impossible. Nevertheless, most of these species probably derived from the samples and not from background or cross contamination, given their much higher abundance as compared to the blank runs. Our results further illustrate that the ratio of organic content to perchlorate controls the degree of thermal degradation during the analyses. As expected, degradation (including chlorination) of organic material increases with the amount of admixed perchlorate (*e.g.,* Fig. 2b, 2c).

4.2.2. *In situ* derivatization. Derivatization with MTBSTFA/DMF (*i.e.,* silylation) can be used for a variety of functional molecules (*e.g.,* acids, alcohols, amines) and is usually producing high analytical responses (Schummer *et al.,* 2009). Indeed, most functional compounds in the standard mixture were successfully silylated via *in situ* derivatization with MTBSTFA/DMF leading to a good GC-MS response. Characteristic key ions (*m/z* 73, 75, M-57, where M denotes the mass of the molecular ion; Schummer *et al.,* 2009) simplified the identification of specific molecules. The lower response of *n*-alkanoic acids (especially *n*-tridecanoic acid) compared to *n*-alkan-2-ols (Fig. S.2) is due to a lower reactivity of *n*-alkanoic acids toward silylation compared to *n*-alkanols (Villas-Bôas *et al.,* 2005, 2007).

In situ DMF-DMA derivatization was developed for use in the COSAC (Cometary Sampling and Composition Experiment) instrument on board the Rosetta lander Philae and is designed for derivatization of alkanoic acids, primary amines and amino acids via methylation (Meierhenrich *et al.,* 2001). However, this technique was unsuccessful for derivatization of *n*-alkanoic acids in our standard mixture. This might be explained by a lower derivatization efficiency of DMF-DMA as compared to MTBSTFA/DMF (Rodier *et al.,* 2001; Meunier *et al.,* 2007; Goesmann *et al.,* 2017), with the latter already giving low responses for *n*-alkanoic acids (see Section 3.3, Fig. S.2a). However, the strength of DMF-DMA lies in its suitability for the analysis of chiral functional molecules (*e.g.,* amino acids), when using it together with an enantioselective column (Freissinet *et al.,* 2010) which was not part of this study.

Earlier analyses revealed that the derivatization techniques are not suited for a sufficient specification of the black chert's organic inventory. This matter is discussed in the work of Goesmann *et al.* (2017; their Chapter 7.5).

Both techniques, MTBSTFA/DMF and DMF-DMA, were not affected by addition of 1 wt % Mg-perchlorates (*e.g.,* Fig. S.2b). Earlier test experiments (not described here) showed that even high amounts of Mg-perchlorate do not have a major detrimental effect on these analyses. This might be explained by the fact that the reaction temperatures of these techniques (250°C and 140°C, respectively) are below the main decomposition temperature of Mg-perchlorate (*i.e.,* release of high amounts of oxygen and chlorine >300°C; Navarro-González *et al.,* 2010, 2011; Sephton *et al.,* 2014). However, potential catalytic effects reducing perchlorate decomposition temperatures have to be considered here (*e.g.,* caused by presence of iron or other metal oxides; Rudloff and Freeman, 1970; Bruck *et al.,* 2014), whose study is beyond the scope of this work. Main decomposition temperatures of other perchlorates likely present on Mars (Ca-, Na-, and K-perchlorate; >390°C, >480°C, and >500°C, respectively) are well above derivatization reaction temperatures (Marvin and Woolaver, 1945; Bircumshaw and Phillips, 1953; Bruck *et al.,* 2014; Kounaves *et al.,* 2014; Sutter *et al.,* 2017b). Hence, it can be assumed that these perchlorates will not affect the analysis of organic compounds via MOMA derivatization techniques.

4.2.3. Thermochemolysis with TMAH: a perchlorate-resistant technique? Thermochemolysis with TMAH combines derivatization and pyrolysis. It can be used for an extraction of organic compounds from mineral matrices and selective cracking of ester and ether bonds from macromolecular organic networks (*i.e.,* kerogen) at elevated temperatures while simultaneously limiting thermal decomposition of organic compounds (Challinor, 2001; Geffroy-Rodier *et al.,* 2009). Compounds from the standard mixture were successfully derivatized by using thermochemolysis (Fig. 4a). The technique revealed higher sensibility for *n*-alkanoic acids in the standard mixture compared to *in situ* derivatization with MTBSTFA/DMF (Fig. 4a; see also Fig. S.2a). However, high abundances of thermal decomposition products (*e.g., n*-alkenes; Fig. 4a) suggest that not all compounds were protected by methylation. One reason for this might be insufficient mixing of TMAH and the sample, so that functional compounds were decomposed at high temperatures before the protecting methylation took place. Additionally, this could have been enhanced by partial evaporation of TMAH at elevated temperatures.

For the black chert, thermochemolysis enabled the detection of *n*-alkanoic acids in addition to the products that

Downloaded by MPI Sonnensystemforschung MPI 359 from www.liebertpub.com at 04/05/20. For personal use only.

were obtained during pyrolysis (Fig. 5a). It is likely that these *n*-alkanoic acids were cleaved from the kerogen and not introduced as contaminants, because they were not observed in pre- and post-analysis blanks.

While most organics in both the standard mix and the black chert were degraded during pyrolysis with up to 10 wt % Mg-perchlorate (Figs. 2c and 3c), they remained largely unaffected during thermochemolysis with TMAH (Figs. 4c and 5b). In the standard mixture, however, a lower abundance of *n*-alkenes and *n*-alkanals as compared to analysis without perchlorate (Fig. 4) might be caused by perchlorate-induced degradation to CO_2 or by variations in the thermal decomposition behavior of parent molecules (see Section 4.1). Likewise, the lower abundance of *n*-alkanoic acids as methyl esters (Fig. 4c) may be explained by slight variations in the efficiency of the methylation reaction. Larger variety and higher abundance of (specific) aromatic hydrocarbons observed in the black chert are probably an effect of perchlorate addition (Fig. 5b).

Our results suggest that TMAH buffers the oxidation and chlorination reactions induced by perchlorate decomposition and thus ''protects'' the organic compounds contained in the samples. We hypothesize that the methyl groups of the tetramethylammonium ion react with the O and Cl radicals via substitution reactions and potentially form, for example, CO_2, HCl, and low-molecular-weight chlorinated organics. As a by-product, this reaction might form dimethylamine, methylamine, or nitrogen radicals which have the potential to produce the abundant nitrogen-bearing organics observed (*e.g.,* 1,5-dicyano-2,4-dimethyl-2,4-diazapentane, benzonitrile; Figs. 4c and 5b). More systematic studies are necessary to determine the exact mechanisms of these reactions.

4.3. Implications for current/future missions

Given the advantages and limits of the individual methods, a complementary use of several techniques seems necessary to obtain a comprehensive picture of the organics contained in a given sample. In this study, especially *in situ* derivatization of the standard mixture with MTBSTFA/DMF and *in situ* thermochemolysis with TMAH have demonstrated good potential for such a complementary analysis. While the former allowed a clear-cut identification of specific compounds (via key ions) without major formation of by-products, the latter revealed the full range of functionalized compounds in proper relative abundances. TMAH furthermore protects the derivatives of *n*-alkanols and *n*-alkanoic acids from thermal decomposition and from the destructive influence of Mg-perchlorates at high temperatures (TMAH buffer). These properties are critical for the search and detection of organic compounds in perchlorate-bearing martian surface material and can be of great use to the ongoing MSL Curiosity as well as the future ExoMars rover mission. Further systematic studies with different perchlorates (Mars-like mixtures) and flight-like derivatization capsules carried out under Mars-like conditions will be necessary to fully validate these results.

5. Summary

MOMA-like pyrolysis, *in situ* derivatization, and thermochemolysis GC-MS techniques were successfully applied on a synthetic sample (standard mix; *n*-alkan-1-ols, *n*-alkan-2-ols, *n*-alkanoic acids) and a natural sample (Silurian black chert). However, not every technique is equally suitable for analyzing different types of organic compounds.

- **Pyrolysis** of synthetic *n*-alkanols and *n*-alkanoic acids at 700°C only yielded their thermal decomposition products (*e.g., n*-alkenes, *n*-alkanals, *n*-alkanones). Meanwhile, pyrolysis of the black chert provided a sufficient overview of its organic inventory. However, high temperatures potentially lead to the production of analytical by-products, for example, aromatic and unsaturated compounds. Furthermore, the impact of high perchlorate concentrations (10 wt %) on pyrolysis was substantial so that organics in the black chert were severely degraded.
- ***In situ* derivatization with MTBSTFA/DMF** resulted in *tert*-butyldimethylsilyl ethers and esters of corresponding *n*-alkanols and *n*-alkanoic acids, respectively, and facilitated their identification due to specific key ions. On the other hand, this technique revealed extremely low abundances of *n*-alkanoic acid derivatives for the standard mixture and only contamination signal for the black chert (see also Goesmann *et al.,* 2017). No impact of perchlorate on the analyses has been observed under the given test conditions.
- The **DMF-DMA derivatization** technique is not applicable to the types of organic compounds present in the used samples.
- ***In situ* thermochemolysis** with TMAH of the standard mixture generated methyl ethers and esters of *n*-alkanols and *n*-alkanoic acids, respectively, in their original abundances. It also revealed the full organic inventory of the black chert. Nevertheless, thermal decomposition products for *n*-alkanols and *n*-alkanoic acids were observed suggesting an incomplete reaction of TMAH with the organic matter of the sample. Up to 10 wt % perchlorate content did not affect the thermochemolysis. We infer that methyl groups from TMAH reacted with O and Cl radicals resulting from perchlorate decomposition, thus buffering the oxidation and chlorination of the organic compounds from the sample.

Summarizing, we demonstrated that perchlorates in martian soils probably do not hinder MOMA-like GC-MS analyses if the effects are carefully considered, and analytical techniques are appropriately adapted for individual target compounds. In particular, we underline that the complementary use of different MOMA-like GC-MS techniques is advantageous to the detection of the full organic inventory of a given sample.

Acknowledgments

We thank Marcus Elvert, two anonymous reviewers, and the associate editor for their helpful comments on the manuscript. We also acknowledge Barbara Kremer and Jósef Kazmierczak (Institute of Paleobiology, Polish Academy of Science) for providing the black chert sample from Holy Cross Mountains, Poland. H.M. gratefully acknowledges his scholarship from the International Max Planck Research School (IMPRS) for Solar System Research, Göttingen. The MOMA project is supported by the Deutsche Zentrum für Luft- und Raumfahrt (DLR grant #50QX1401).

Downloaded by MPI Sonnensystemforschung MPI 359 from www.liebertpub.com at 04/05/20. For personal use only.

References

Bibring, J.-P., Hamm, V., Pilorget, C., Vago, J.L., and the MicrOmega Team. (2017) The MicrOmega investigation on board ExoMars. *Astrobiology* 17:621–626.

Biemann, K. and Bada, J.L. (2011) Comment on ''Reanalysis of the Viking results suggests perchlorate and organics at mid-latitudes on Mars'' by Rafael Navarro-González *et al. J Geophys Res Planets* 116, doi:10.1029/2010JE003599.

Biemann, K., Oró, J., Toulmin, P., Orgel, L.E., Nier, A.O., Anderson, D.M., Simmonds, P.G., Flory, D., Diaz, A.V., Rushneck, D.R., and Biller, J.A. (1976) Search for organic and volatile inorganic compounds in two surface samples from the Chryse Planitia region of Mars. *Science* 194:72–76.

Biemann, K., Oró, J., Toulmin, P., Orgel, L.E., Nier, A.O., Anderson, D.M., Simmonds, P.G., Flory, D., Diaz, A.V., Rushneck, D.R., Biller, J.E., and Lafleur, A.L. (1977) The search for organic substances and inorganic volatile compounds in the surface of Mars. *J Geophys Res* 82:4641–4658.

Bircumshaw, L.L. and Phillips, T.R. (1953) The thermal decomposition of potassium perchlorate. *J Am Chem Soc* 142: 703–707.

Boss, B.D. and Hazlett, R.N. (1976) Application of pyrolysis, gas chromatography, and mass spectrometry for identification of alcohol and carbonyl isomers. *Anal Chem* 48:417–420.

Botta, O. and Bada, J.L. (2002) Extraterrestrial organic compounds in meteorites. *Surv Geophys* 23:411–467.

Bridges, J.C., Loizeau, D., Sefton-Nash, E., Vago, J., Williams, R.M.E., Balme, M., Turner, S.M.R., Fawdon, P., Davis, J.M., and the ExoMars Landing Site Selection Working Group. (2017) Selection and characterisation of the ExoMars 2020 rover landing sites [abstract 2378]. In *48th Lunar and Planetary Science Conference Abstracts,* Lunar and Planetary Institute, Houston.

Brocks, J.J. and Summons, R.E. (2004) Biomarkers for early life. In *Biogeochemistry*, edited by W.H. Schlesinger, Elsevier, Oxford, UK, pp 63–115.

Brown, G.M. and Gu, B. (2006) The chemistry of perchlorate in the environment. In *Perchlorate: Environmental Occurrence, Interactions and Treatment,* edited by B. Gu and J.D. Coates, Springer US, Boston, MA, pp 17–47.

Bruck, A.M., Sutter, B., Ming, D.W., and Mahaffy, P. (2014) Thermal decomposition of calcium perchlorate/iron-mineral mixtures: implications of the evolved oxygen from the Rocknest eolian deposit in Gale Crater, Mars [abstract 2057]. In *45th Lunar and Planetary Science Conference Abstracts,* Lunar and Planetary Institute, Houston.

Buch, A., Glavin, D.P., Sternberg, R., Szopa, C., Rodier, C., Navarro-González, R., Raulin, F., Cabane, M., and Mahaffy, P.R. (2006) A new extraction technique for *in situ* analyses of amino and carboxylic acids on Mars by gas chromatography mass spectrometry. *Planet Space Sci* 54:1592–1599.

Burnham, A.K., Clarkson, J.E., Singleton, M.F., Wong, C.M., and Crawford, R.W. (1982) Biological markers from Green River kerogen decomposition. *Geochim Cosmochim Acta* 46: 1243–1251.

Cady, S.L. and Noffke, N. (2009) Geobiology: evidence for early life on Earth and the search for life on other planets. *GSA Today* 19:4–10.

Carter, J., Quantin, C., Thollot, P., Loizeau, D., Ody, A., and Lozach, L. (2016) Oxia Planum, a clay-laden landing site proposed for the ExoMars rover mission: aqueous mineralogy and alteration scenarios [abstract 2064]. In *47th Lunar and Planetary Science Conference Abstracts,* Lunar and Planetary Institute, Houston.

Catling, D.C., Claire, M.W., Zahnle, K.J., Quinn, R.C., Clark, B.C., Hecht, M.H., and Kounaves, S. (2010) Atmospheric origins of perchlorate on Mars and in the Atacama. *J Geophys Res Planets* 115, doi:10.1029/2009JE003425.

Challinor, J.M. (2001) Review: the development and applications of thermally assisted hydrolysis and methylation reactions. *J Anal Appl Pyrolysis* 61:3–34.

Cull, S.C., Arvidson, R.E., Catalano, J.G., Ming, D.W., Morris, R.V., Mellon, M.T., and Lemmon, M. (2010) Concentrated perchlorate at the Mars Phoenix landing site: evidence for thin film liquid water on Mars. *Geophys Res Lett* 37, doi: 10.1029/2010GL045269.

Duda, J.P., Van Kranendonk, M.J., Thiel, V., Ionescu, D., Strauss, H., Schäfer, N., and Reitner, J. (2016) A rare glimpse of Paleoarchean life: geobiology of an exceptionally preserved microbial mat facies from the 3.4 Ga Strelley Pool Formation, Western Australia. *PloS One* 11, doi:10.1371/journal.pone.0147629.

Duda, J.P., Thiel, V., Bauersachs, T., Mißbach, H., Reinhardt, M., Schäfer, N., Van Kranendonk, M.J., and Reitner, J. (2018) Ideas and perspectives: hydrothermally driven redistribution and sequestration of early Archaean biomass—the ''hydrothermal pump hypothesis.'' *Biogeosciences* 15:1535–1548.

Eigenbrode, J.L., Summons, R.E., Steele, A., Freissinet, C., Millan, M., Navarro-González, R., Sutter, B., McAdam, A.C., Franz, H.B., Glavin, D.P., Archer, P.D., Mahaffy, P.R., Conrad, P.G., Hurowitz, J.A., Grotzinger, J.P., Gupta, S., Ming, D.W., Sumner, D.Y., Szopa, C., Malespin, C., Buch, A., and Coll, P. (2018) Organic matter preserved in 3-billion-year-old mudstones at Gale Crater, Mars. *Science* 360:1096–1101.

Flynn, G.J. (1996) The delivery of organic matter from asteroids and comets to the early surface of Mars. *Earth Moon Planets* 72:469–474.

Freissinet, C., Buch, A., Sternberg, R., Szopa, C., Geffroy-Rodier, C., Jelinek, C., and Stambouli, M. (2010) Search for evidence of life in space: analysis of enantiomeric organic molecules by *N,N*-dimethylformamide dimethylacetal derivative dependant gas chromatography–mass spectrometry. *Journal of Chromatography A* 1217:731–740.

Freissinet, C., Glavin, D.P., Mahaffy, P.R., Miller, K.E., Eigenbrode, J.L., Summons, R.E., Brunner, A.E., Buch, A., Szopa, C., Archer, P.D., Franz, H.B., Atreya, S.K., Brinckerhoff, W.B., Cabane, M., Coll, P., Conrad, P.G., Des Marais, D.J., Dworkin, J.P., Fairén, A.G., François, P., Grotzinger, J.P., Kashyap, S., ten Kate, I.L., Leshin, L.A., Malespin, C.A., Martin, M.G., Martin-Torres, F.J., McAdam, A.C., Ming, D.W., Navarro-González, R., Pavlov, A.A., Prats, B.D., Squyres, S.W., Steele, A., Stern, J.C., Sumner, D.Y., Sutter, B., Zorzano, M.P., and the MSL Science Team. (2015) Organic molecules in the Sheepbed Mudstone, Gale Crater, Mars. *J Geophys Res Planets* 120:495–514.

Geffroy-Rodier, C., Grasset, L., Sternberg, R., Buch, A., and Amblès, A. (2009) Thermochemolysis in search for organics in extraterrestrial environments. *J Anal Appl Pyrolysis* 85: 454–459.

Glavin, D.P., Freissinet, C., Miller, K.E., Eigenbrode, J.L., Brunner, A.E., Buch, A., Sutter, B., Archer, P.D., Atreya, S.K., Brinckerhoff, W.B., Cabane, M., Coll, P., Conrad, P.G., Coscia, D., Dworkin, J.P., Franz, H.B., Grotzinger, J.P., Leshin, L.A., Martin, M.G., McKay, C., Ming, D.W., Navarro-González, R., Pavlov, A., Steele, A., Summons, R.E., Szopa, C., Teinturier, S., and Mahaffy, P.R. (2013) Evidence for

Downloaded by MPI Sonnensystemforschung MPI 359 from www.liebertpub.com at 04/05/20. For personal use only.

perchlorates and the origin of chlorinated hydrocarbons detected by SAM at the Rocknest aeolian deposit in Gale Crater. *J Geophys Res Planets* 118:1955–1973.

Goesmann, F., Brinckerhoff, W.B., Raulin, F., Goetz, W., Danell, R.M., Getty, S.A., Siljeström, S., Mißbach, H., Steininger, H., Arevalo, R.D., Buch, A., Freissinet, C., Grubisic, A., Meierhenrich, U.J., Pinnick, V.T., Stalport, F., Szopa, C., Vago, J.L., Lindner, R., Schulte, M.D., Brucato, J.R., Glavin, D.P., Grand, N., Li, X., van Amerom, F.H.W., and the MOMA Science Team. (2017) The Mars Organic Molecule Analyzer (MOMA) instrument: characterization of organic material in martian sediments. *Astrobiology* 17:655–685.

Goetz, W., Brinckerhoff, W.B., Arevalo, R., Freissinet, C., Getty, S., Glavin, D.P., Siljeström, S., Buch, A., Stalport, F., Grubisic, A., Li, X., Pinnick, V., Danell, R., van Amerom, F.H.W., Goesmann, F., Steininger, H., Grand, N., Raulin, F., Szopa, C., Meierhenrich, U., and Brucato, J.R. (2016) MOMA: the challenge to search for organics and biosignatures on Mars. *Int J Astrobiol* 15:239–250.

Guzman, M., McKay, C.P., Quinn, R.C., Szopa, C., Davila, A.F., Navarro-González, R., and Freissinet, C. (2018) Identification of chlorobenzene in the Viking gas chromatograph–mass spectrometer data sets: reanalysis of Viking mission data consistent with aromatic organic compounds on Mars. *J Geophys Res Planets* 123:1674–1683.

Hallmann, C., Kelly, A.E., Gupta, S.N., and Summons, R.E. (2011) Reconstructing deep-time biology with molecular fossils. In *Quantifying the Evolution of Early Life,* edited by M. Laflamme, J.D. Schiffbauer, and S.Q. Dornbos, Springer, Dordrecht, the Netherlands, pp 355–401.

Hartgers, W.A., Sinninghe Damsté, J.S., and de Leeuw, J.W. (1994) Geochemical significance of alkylbenzene distributions in flash pyrolysates of kerogens, coals, and asphaltenes. *Geochim Cosmochim Acta* 58:1759–1775.

Hartgers, W.A., Sinninghe Damsté, J.S., and de Leeuw, J.W. (1995) Curie-point pyrolysis of sodium salts of functionalized fatty acids. *J Anal Appl Pyrolysis* 34:191–217.

Hecht, M.H., Kounaves, S.P., Quinn, R.C., West, S.J., Young, S.M.M., Ming, D.W., Catling, D.C., Clark, B.C., Boynton, W.V., Hoffman, J., DeFlores, L.P., Gospodinova, K., Kapit, J., and Smith, P.H. (2009) Detection of perchlorate and the soluble chemistry of martian soil at the Phoenix lander site. *Science* 325:64–67.

Huizinga, B.J., Aizenshtat, Z.A., and Peters, K.E. (1988) Programmed pyrolysis–gas chromatography of artificially matured Green River kerogen. *Energy & Fuels* 2:74–81.

Kminek, G. and Bada, J.L. (2006) The effect of ionizing radiation on the preservation of amino acids on Mars. *Earth Planet Sci Lett* 245:1–5.

Konn, C., Charlou, J.L., Holm, N.G., and Mousis, O. (2015) The production of methane, hydrogen, and organic compounds in ultramafic-hosted hydrothermal vents of the Mid-Atlantic Ridge. *Astrobiology* 15:381–399.

Kounaves, S.P., Hecht, M.H., Kapit, J., Gospodinova, K., DeFlores, L., Quinn, R.C., Boynton, W.V., Clark, B.C., Catling, D.C., Hredzak, P., Ming, D.W., Moore, Q., Shusterman, J., Stroble, S., West, S.J., and Young, S.M.M. (2010) Wet chemistry experiments on the 2007 Phoenix Mars Scout lander mission: data analysis and results. *J Geophys Res Planets* 115, doi:10.1029/2009JE003424.

Kounaves, S.P., Chaniotakis, N.A., Chevrier, V.F., Carrier, B.L., Folds, K.E., Hansen, V.M., McElhoney, K.M., O'Neil, G.D., and Weber, A.W. (2014) Identification of the perchlorate parent salts at the Phoenix Mars landing site and possible implications. *Icarus* 232:226–231.

Kremer, B. (2005) Mazuelloids: product of post-mortem phosphatization of acanthomorphic acritarchs. *Palaios* 20:27–36.

Kremer, B. and Kazmierczak, J. (2005) Cyanobacterial mats from Silurian black radiolarian cherts: phototrophic life at the edge of darkness? *Journal of Sedimentary Research* 75:897–906.

Levin, G.V. and Straat, P.A. (2016) The case for extant life on Mars and its possible detection by the Viking Labeled Release experiment. *Astrobiology* 16:798–810.

Lewan, M.D., Winters, J.C., and McDonald, J.H. (1979) Generation of oil-like pyrolyzates from organic-rich shales. *Science* 203:897–899.

Li, X., Danell, R.M., Pinnick, V.T., Grubisic, A., van Amerom, F., Arevalo, R.D., Getty, S.A., Brinckerhoff, W.B., Southard, A.E., Gonnsen, Z.D., and Adachi, T. (2017) Mars Organic Molecule Analyzer (MOMA) laser desorption/ionization source design and performance characterization. *Int J Mass Spectrom* 422:177–187.

Lockhart, T.P., Comita, P.B., and Bergman, R.G. (1981) Kinetic evidence for the formation of discrete 1, 4-dehydrobenzene intermediates. Trapping by inter-and intramolecular hydrogen atom transfer and observation of high-temperature CIDNP. *J Am Chem Soc* 103:4082–4090.

Mahaffy, P.R., Webster, C.R., Cabane, M., Conrad, P.G., Coll, P., Atreya, S.K., Arvey, R., Barciniak, M., Benna, M., Bleacher, L., Brinckerhoff, W.B., Eigenbrode, J.L., Carignan, D., Cascia, M., Chalmers, R.A., Dworkin, J.P., Errigo, T., Everson, P., Franz, H., Farley, R., Feng, S., Frazier, G., Freissinet, C., Glavin, D.P., Harpold, D.N., Hawk, D., Holmes, V., Johnson, C.S., Jones, A., Jordan, P., Kellogg, J., Lewis, J., Lyness, E., Malespin, C.A., Martin, D.K., Maurer, J., McAdam, A.C., McLennan, D., Nolan, T.J., Noriega, M., Pavlov, A.A., Prats, B., Raaen, E., Sheinman, O., Sheppard, D., Smith, J., Stern, J.C., Tan, F., Trainer, M., Ming, D.W., Morris, R.V., Jones, J., Gundersen, C., Steele, A., Wray, J., Botta, O., Leshin, L.A., Owen, T., Battel, S., Jakosky, B.M., Manning, H., Squyres, S., Navarro-González, R., McKay, C.P., Raulin, F., Sternberg, R., Buch, A., Sorensen, P., Kline-Schoder, R., Coscia, D., Szopa, C., Teinturier, S., Baffes, C., Feldman, J., Flesch, G., Forouhar, S., Garcia, R., Keymeulen, D., Woodward, S., Block, B.P., Arnett, K., Miller, R., Edmonson, C., Gorevan, S., and Mumm, E. (2012) The Sample Analysis at Mars investigation and instrument suite. *Space Sci Rev* 170:401–478.

Manelis, G., Nazin, G., Rubtsov, Y., and Strunin, V. (2003) *Thermal Decomposition and Combustion of Explosives and Propellants,* Taylor & Francis, London.

Marshall, C.P., Love, G.D., Snape, C.E., Hill, A.C., Allwood, A.C., Walter, M.R., Van Kranendonk, M.J., Bowden, S.A., Sylva, S.P., and Summons, R.E. (2007) Structural characterization of kerogen in 3.4 Ga Archaean cherts from the Pilbara Craton, Western Australia. *Precambrian Res* 155:1–23.

Martín-Torres, F.J., Zorzano, M.-P., Valentín-Serrano, P., Harri, A.-M., Genzer, M., Kemppinen, O., Rivera-Valentin, E.G., Jun, I., Wray, J., Bo Madsen, M., Goetz, W., McEwen, A.S., Hardgrove, C., Renno, N., Chevrier, V.F., Mischna, M., Navarro-González, R., Martínez-Frías, J., Conrad, P., McConnochie, T., Cockell, C., Berger, G.R., Vasavada, A., Sumner, D., and Vaniman, D. (2015) Transient liquid water and water activity at Gale Crater on Mars. *Nat Geosci* 8:357–361.

Marvin, G.G. and Woolaver, L.B. (1945) Thermal decomposition of perchlorates. *Industrial and Engineering Chemistry Analytical Edition* 17:474–476.

McCollom, T.M. and Seewald, J.S. (2007) Abiotic synthesis of organic compounds in deep-sea hydrothermal environments. *Chem Rev* 107:382–401.

McCollom, T.M., Ritter, G., and Simoneit, B.R.T. (1999) Lipid synthesis under hydrothermal conditions by Fischer–Tropsch-type reactions. *Orig Life Evol Biosph* 29:153–166.

Meierhenrich, U. (2008) *Amino Acids and the Asymmetry of Life: Caught in the Act of Formation,* Springer Science & Business Media, Berlin.

Meierhenrich, U., Thiemann, W.H.P., and Rosenbauer, H. (2001) Pyrolytic methylation assisted enantioseparation of chiral hydroxycarboxylic acids. *J Anal Appl Pyrolysis* 60:13–26.

Meunier, D., Sternberg, R., Mettetal, F., Buch, A., Coscia, D., Szopa, C., Rodier, C., Coll, P., Cabanec, M., and Raulin, F. (2007) A laboratory pilot for *in situ* analysis of refractory organic matter in martian soil by gas chromatography–mass spectrometry. *Adv Space Res* 39:337–344.

Mißbach, H., Duda, J.-P., Lünsdorf, N.K., Schmidt, B.C., and Thiel, V. (2016) Testing the preservation of biomarkers during experimental maturation of an immature kerogen. *Int J Astrobiol* 15:165–175.

Mißbach, H., Schmidt, B.C., Duda, J.-P., Lünsdorf, N.K., Goetz, W., and Thiel, V. (2018) Assessing the diversity of lipids formed via Fischer–Tropsch-type reactions. *Org Geochem* 119:110–121.

Moldoveanu, S.C. (2010) *Pyrolysis of Organic Molecules with Applications to Health and Environmental Issues,* Elsevier Science, Amsterdam.

Morisson, M. (2017) *Optimisation des Techniques de Pyrolyse et de Thermochimiolyse pour la Recherche de Matière Organique d'Origine Extraterrestre: Application aux cas de Titan et Mars,* Université Paris-Saclay, Paris.

Navarro-González, R. and McKay, C.P. (2011) Reply to comment by Biemann and Bada on ''Reanalysis of the Viking results suggests perchlorate and organics at midlatitudes on Mars.'' *J Geophys Res Planets* 116, doi:10.1029/2011JE003869.

Navarro-González, R., Vargas, E., de la Rosa, J., Raga, A.C., and McKay, C.P. (2010) Reanalysis of the Viking results suggests perchlorate and organics at midlatitudes on Mars. *J Geophys Res Planets* 115, doi:10.1029/2010JE003599.

Navarro-González, R., Vargas, E., de la Rosa, J., Raga, A.C., and McKay, C.P. (2011) Correction to ''Reanalysis of the Viking results suggests perchlorate and organics at midlatitudes on Mars.'' *J Geophys Res Planets* 116, doi:10.1029/2011JE003854.

Nierop, K.G.J. and van Bergen, P.F. (2002) Clay and ammonium catalyzed reactions of alkanols, alkanoic acids and esters under flash pyrolytic conditions. *J Anal Appl Pyrolysis* 63:197–208.

Oró, J. and Holzer, G. (1979) The photolytic degradation and oxidation of organic compounds under simulated martian conditions. *J Mol Evol* 14:153–160.

Pavlov, A.A., Vasilyev, G., Ostryakov, V.M., Pavlov, A.K., and Mahaffy, P. (2012) Degradation of the organic molecules in the shallow subsurface of Mars due to irradiation by cosmic rays. *Geophys Res Lett* 39, doi:10.1029/2012GL052166.

Peters, K.E., Walters, C.C., and Moldowan, J.M. (2005) *The Biomarker Guide—Part II—Biomarkers and Isotopes in Petroleum Exploration and Earth History,* Cambridge University Press, New York.

Rodier, C., Sternberg, R., Raulin, F., and Vidal-Madjar, C. (2001) Chemical derivatization of amino acids for *in situ* analysis of martian samples by gas chromatography. *Journal of Chromatography A* 915:199–207.

Rodier, C., Sternberg, R., Szopa, C., Buch, A., Cabane, M., and Raulin, F. (2005) Search for organics in extraterrestrial environments by *in situ* gas chromatography analysis. *Adv Space Res* 36:195–200.

Rudloff, W.K. and Freeman, E.S. (1970) Catalytic effect of metal oxides on thermal decomposition reactions. II. Catalytic effect of metal oxides on the thermal decomposition of potassium chlorate and potassium perchlorate as detected by thermal analysis methods. *J Phys Chem* 74:3317–3324.

Rull, F., Maurice, S., Hutchinson, I., Moral, A., Perez, C., Diaz, C., Colombo, M., Belenguer, T., Lopez-Reyes, G., Sansano, A., Forni, O., Parot, Y., Striebig, N., Woodward, S., Howe, C., Tarcea, N., Rodriguez, P., Seoane, L., Santiago, A., Rodriguez-Prieto, J.A., Medina, J., Gallego, P., Canchal, R., Santamaría, P., Ramos, G., Vago, J.L., and on behalf of the RLS Team. (2017) The Raman Laser Spectrometer for the ExoMars rover mission to Mars. *Astrobiology* 17:627–654.

Rushdi, A.I. and Simoneit, B.R. (2001) Lipid formation by aqueous Fischer–Tropsch-type synthesis over a temperature range of 100 to 400°C. *Orig Life Evol Biosph* 31:103–118.

Schummer, C., Delhomme, O., Appenzeller, B.M.R., Wennig, R., and Millet, M. (2009) Comparison of MTBSTFA and BSTFA in derivatization reactions of polar compounds prior to GC/MS analysis. *Talanta* 77:1473–1482.

Sephton, M.A., Lewis, J.M.T., Watson, J.S., Montgomery, W., and Garnier, C. (2014) Perchlorate-induced combustion of organic matter with variable molecular weights: implications for Mars missions. *Geophys Res Lett* 41:7453–7460.

Shock, E.L. and Schulte, M.D. (1998) Organic synthesis during fluid mixing in hydrothermal systems. *J Geophys Res Planets* 103:28513–28527.

Steininger, H., Goesmann, F., and Goetz, W. (2012) Influence of magnesium perchlorate on the pyrolysis of organic compounds in Mars analogue soils. *Planet Space Sci* 71:9–17.

Summons, R.E. (2014) The exceptional preservation of interesting and informative biomolecules. In *Reading and Writing of the Fossil Record: Preservational Pathways to Exceptional Fossilization. The Paleontological Society Papers Vol. 20,* edited by M. Laflamme, J.D. Schiffbauer, and S.A.F. Darroch, The Paleontological Society (2014), Bethesda, MD, pp 217–236.

Summons, R.E., Albrecht, P., McDonald, G., and Moldowan, J.M. (2008) Molecular biosignatures. *Space Sci Rev* 135:133–159.

Summons, R.E., Amend, J.P., Bish, D., Buick, R., Cody, G.D., Des Marais, D.J., Dromart, G., Eigenbrode, J.L., Knoll, A.H., and Sumner, D.Y. (2011) Preservation of martian organic and environmental records: final report of the Mars Biosignature Working Group. *Astrobiology* 11:157–181.

Sutter, B., Boynton, W.V., Ming, D.W., Niles, P.B., Morris, R.V., Golden, D.C., Lauer, H.V., Fellows, C., Hamara, D.K., and Mertzman, S.A. (2012) The detection of carbonate in the martian soil at the Phoenix landing site: a laboratory investigation and comparison with the Thermal and Evolved Gas Analyzer (TEGA) data. *Icarus* 218:290–296.

Sutter, B., McAdam, A.C., Mahaffy, P.R., Ming, D.W., Edgett, K.S., Rampe, E.B., Eigenbrode, J.L., Franz, H.B., Freissinet, C., Grotzinger, J.P., Steele, A., House, C.H., Archer, P.D., Malespin, C.A., Navarro-González, R., Stern, J.C., Bell, J.F., Calef, F.J., Gellert, R., Glavin, D.P., Thompson, L.M., and

Downloaded by MPI Sonnensystemforschung MPI 359 from www.liebertpub.com at 04/05/20. For personal use only.

Yen, A.S. (2017a) Evolved gas analyses of sedimentary rocks and eolian sediment in Gale Crater, Mars: results of the Curiosity rover's Sample Analysis at Mars instrument from Yellowknife Bay to the Namib Dune. *J Geophys Res Planets* 122:2574–2609.

Sutter, B., Quinn, R.C., Archer, P.D., Glavin, D.P., Glotch, T.D., Kounaves, S.P., Osterloo, M.M., Rampe, E.B., and Ming, D.W. (2017b) Measurements of oxychlorine species on Mars. *Int J Astrobiol* 16:203–217.

ten Kate, I.L. (2010) Organics on Mars? *Astrobiology* 10:589–603.

Vago, J.L., Westall, F., Coates, A.J., Jaumann, R., Korablev, O., Ciarletti, V., Mitrofanov, I., Josset, J.-L., De Sanctis, M.C., Bibring, J.-P., Rull, F., Goesmann, F., Steininger, H., Goetz, W., Brinckerhoff, W., Szopa, C., Raulin, F., Edwards, H.G.M., Whyte, L.G., Fairén, A.G., Bridges, J., Hauber, E., Ori, G.G., Werner, S., Loizeau, D., Kuzmin, R.O., Williams, R.M.E., Flahaut, J., Forget, F., Rodionov, D., Svedhem, H., Sefton-Nash, E., Kminek, G., Lorenzoni, L., Joudrier, L., Mikhailov, V., Zashchirinskiy, A., Alexashkin, S., Calantropio, F., Merlo, A., Poulakis, P., Witasse, O., Bayle, O., Bayón, S., Meierhenrich, U., Carter, J., García-Ruiz, J.M., Baglioni, P., Haldemann, A., Ball, A.J., Debus, A., Lindner, R., Haessig, F., Monteiro, D., Trautner, R., Voland, C., Rebeyre, P., Goulty, D., Didot, F., Durrant, S., Zekri, E., Koschny, D., Toni, A., Visentin, G., Zwick, M., van Winnendael, M., Azkarate, M., Carreau, C., and the ExoMars Project Team. (2017) Habitability on early Mars and the search for biosignatures with the ExoMars rover. *Astrobiology* 17: 471–510.

Vandenbroucke, M. and Largeau, C. (2007) Kerogen origin, evolution and structure. *Org Geochem* 38:719–833.

Villas-Bôas, S.G., Mas, S., Åkesson, M., Smedsgaard, J., and Nielsen, J. (2005) Mass spectrometry in metabolome analysis. *Mass Spectrom Rev* 24:613–646.

Villas-Bôas, S.G., Koulman, A., and Lane, G.A. (2007) Analytical methods from the perspective of method standardization. In *Metabolomics,* edited by J. Nielsen and M.C. Jewett, Springer, Berlin, pp 11–52.

Westall, F., Foucher, F., Bost, N., Bertrand, M., Loizeau, D., Vago, J.L., Kminek, G., Gaboyer, F., Campbell, K.A., Bréhéret, J.-G., Gautret, P., and Cockell, C.S. (2015) Biosignatures on Mars: what, where, and how? Implications for the search for martian life. *Astrobiology* 15:998–1029.

Zaikin, V. and Halket, J.M. (2009) *A Handbook of Derivatives for Mass Spectrometry,* IM Publications, Chichester, UK.

Address correspondence to:
Helge Mißbach
Geobiology, Geoscience Centre
University of Goettingen
Goldschmidtstraße 3
37077 Goettingen
Germany

E-mail: hmissba@gwdg.de

Submitted 7 December 2018
Accepted 20 July 2019
Associate Editor: Victor Parro

Abbreviations Used

DMF = *N,N*-dimethylformamide
DMF-DMA = *N,N*-dimethylformamide dimethyl acetal
FAS = flight analog system
GC = gas chromatograph
GC-MS = gas chromatography–mass spectrometry
MOMA = Mars Organic Molecule Analyzer
MS = mass spectrometer
MSL = Mars Science Laboratory
MTBSTFA = *N,N*-methyl-tert-butyl-dimethylsilyltrifluoroacetamide
SAM = Sample Analysis at Mars
TMAH = tetramethylammonium hydroxide

Downloaded by MPI Sonnensystemforschung MPI 359 from www.liebertpub.com at 04/05/20. For personal use only.